Plant Communications
Research Article

CellPress
Partner Journal

Two MADS-box genes regulate vascular cambium activity and secondary growth by modulating auxin homeostasis in *Populus*

Shuai Zheng[1,2], Jiajia He[1,2], Zengshun Lin[3], Yingying Zhu[4], Jiayan Sun[1] and Laigeng Li[1,*]

[1]National Key Laboratory of Plant Molecular Genetics and CAS Center for Excellence in Molecular Plant Sciences, Institute of Plant Physiology and Ecology, Chinese Academy of Sciences, Shanghai 200032, China

[2]University of the Chinese Academy of Sciences, Beijing 100049, China

[3]Hunan Agricultural University, Hunan 4101287, China

[4]Lanzhou University, Lanzhou, 730000, China

***Correspondence: Laigeng Li (lgli@sibs.ac.cn)**

https://doi.org/10.1016/j.xplc.2020.100134

ABSTRACT

In trees, stem secondary growth depends on vascular cambium proliferation activity and subsequent cell differentiation, in which an auxin concentration gradient across the cambium area plays a crucial role in regulating the process. However, the underlying molecular mechanism for the establishment of auxin concentration is not fully understood. In this study, we identified two function-unknown MADS-box genes, *VCM1* and *VCM2*, which are expressed specifically in the vascular cambium and modulate the subcellular homeostasis of auxin. Simultaneous knockdown of both *VCM1* and *VCM2* enhanced vascular cambium proliferation activity and subsequent xylem differentiation. Overexpression of *VCM1* suppressed vascular cambium activity and wood formation by regulating *PIN5* expression, which tuned the soluble auxin concentration in the vascular cambium area. This study reveals the role of *VCM1* and *VCM2* in regulating the proliferation activity of the vascular cambium and secondary growth by modulating the subcellular auxin homeostasis in *Populus*.

Key words: vascular cambium, secondary growth, auxin, xylem, tree

Zheng S., He J., Lin Z., Zhu Y., Sun J., and Li L. (2021). Two MADS-box genes regulate vascular cambium activity and secondary growth by modulating auxin homeostasis in *Populus*. Plant Comm. **2**, 100134.

INTRODUCTION

Unlike herbaceous plants, woody plants feature perennial secondary growth, which gives rise to radial increments of the stem. Secondary growth is dependent on the activity of the vascular cambium, which divides and produces daughter cells that subsequently differentiate into secondary vascular tissues with phloem cells on the outside and xylem cells on the inside (wood tissue). During this process, a set of sequential events, including cell division, cell fate determination, and cell differentiation, are modulated through a complex of signaling networks (Spicer and Groover, 2010; Campbell and Turner, 2017; Fischer et al., 2019). Studies have reported the involvement of auxin in regulating vascular cambium activity and the secondary growth of stem. Auxin supplied to stem tissues stimulates cambial growth and mediates multiple aspects of xylem development (Bjorklund et al., 2007; Johnsson et al., 2019). Modulations of auxin transport and responsive genes regulate wood formation in the annual growth of trees (Moyle et al., 2002; Schrader et al., 2004; Baba et al., 2011). Auxin-responsive genes respond dynamically to changes in cellular auxin levels in wood-forming tissues (Nilsson et al., 2008). During the secondary growth of stem in trees, indole-3-acetic acid (IAA) and its derivatives form a concentration gradient cross the vascular cambial zone, with an IAA peak in the cambium area (Uggla et al., 1996, 1998). The peak height and the radial width of IAA distribution play a crucial role in determining cambium activity and xylem differentiation during wood formation (Tuominen et al., 1997). However, it is unknown how IAA concentration is maintained and regulated during the secondary growth of stem.

The establishment of cellular auxin concentration can be attributed to polar auxin transport, intracellular auxin homeostasis, and metabolic processes (Park et al., 2017). In *Arabidopsis thaliana*, it is known that auxin can be translocated by several

Published by the Plant Communications Shanghai Editorial Office in association with Cell Press, an imprint of Elsevier Inc., on behalf of CSPB and IPPE, CAS.

types of transporters, including pin-formed proteins (PIN), proteins of the auxin transporter protein 1 (AUX1), auxin transporter-like protein (LAX), P-glycoproteins (PGP) of the ATP-binding cassette (ABC) transporter family, and pin-likes (PILS) (Grones and Friml, 2015). These transporters perform their functions in different manners. Most PIN proteins are located at particular plasma membrane regions for directional auxin transport (Petrasek et al., 2006; Wisniewska et al., 2006). However, PIN5 is localized at the endoplasmic reticulum (ER), and it is suggested to control cellular auxin homeostasis by transporting auxin from the cytosol to the ER lumen, which decreases the cellular level of free IAA (Mravec et al., 2009). It is believed that PIN5-dependent transport limits the availability of cytosolic auxin for signaling (Ding et al., 2012). The *Populus* genome contains three PIN5 homologs, of which two members are highly expressed in the stem, showing localization at the ER (Liu et al., 2014). It is unclear whether the *Populus PIN5* homologs function in tuning the cellular auxin level in the stem.

MADS-box transcription factors have active roles in all major developmental processes throughout the entire life cycle of land plants (Gramzow and Theissen, 2010). For example, several MADS-box transcription factor genes are known for their involvement in regulating meristem activity, floral organ identity specification, and organ development (Dornelas et al., 2011). In plants, there is a large family of genes encoding MADS-box transcription factors. The *Arabidopsis* genome contains 107 MADS-box genes (Parenicova et al., 2003). Seventy-five MADS-box genes are present in rice (Arora et al., 2007). In the *Populus* genome, there are 105 putative MADS-box genes and 12 pseudogenes with a MADS-box structure (Leseberg et al., 2006). However, the function of most MADS-box genes is unknown.

In our previous work, the regulation of *PtrHB4* expression caused serious defects during vascular cambium development in *Populus* (Zhu et al., 2018). In the defective vascular cambium, the expression of a group of MADS-box genes was extensively modified. In this study, we show evidence demonstrating that two MADS-box genes, *VCM1* and *VCM2*, play a role in regulating the secondary growth of stem in *Populus*. We carried out a genetic analysis to show that *VCM1* and *VCM2* affect vascular cambium proliferation activity. Further genomic and cellular analyses revealed that *VCM1* and *VCM2* regulate *PIN5b* expression, which in turn modulates the homeostasis of phytohormone auxin. Our study suggests that *VCM1* and *VCM2* play a role in regulating the secondary growth of stem through PIN5-mediated subcellular auxin transport, which tunes cytosolic auxin levels across the vascular cambium area.

RESULTS

Identification of regulatory genes of vascular cambium activity in *Populus*

In our previous study, the suppression of *PtrHB4* caused defects in the *Populus* vascular cambium (Zhu et al., 2018). The defective vascular cambium tissue in the *PtrHB4*-suppressed *Populus* was subjected to RNA sequencing, and transcriptome analysis revealed that the expression of a group of transcription factor genes was substantially altered (Supplemental Table 1), suggesting that transcriptional regulatory networks were modified in the defective vascular cambium. Further analysis showed that the regulated transcription factors included two homologous function-unknown MADS-box genes, Potri.012G100200 and Potri.015G098400. Interestingly, when they were searched in the Nucleotide Database (https://blast.ncbi.nlm.nih.gov), their homologs were identified primarily in woody plant species (Supplemental Figure 1A). Subsequently, the homologs of Potri.012G100200 and Potri.015G098400 were cloned from *Populus deltoides* × *P. euramericana* cv. ''Nanlin895'' (Supplemental Figure 1B). Quantitative transcript analysis showed that their expression was specific in stem tissues undergoing secondary growth (IN9 and IN10) (Figure 1A and 1B). Thus, the two genes, Potri.012G100200 and Potri.015G098400, were named *Vascular Cambium-related MADS* 1 and 2 (*VCM1* and *VCM2*), respectively. VCM1 and VCM2 share a 73.3% identity in protein sequence (Supplemental Figure 1C). Next, we cloned *VCM1* and *VCM2* promoter fragments and transferred the promoter-GUS constructs into *Populus* to further examine their expression location. GUS activity was detected in the vascular cambium area, including the cambium and developing phloem and xylem cells (Figure 1C and 1D). These results indicate that the expression of *VCM1* and *VCM2* is closely correlated with the process of secondary growth in *Populus*.

Down- or upregulation of *VCM1* and *VCM2* expression leads to abnormal secondary growth

To examine the genetic function of *VCM1* and *VCM2*, we carried out knockdowns of their expression in *Populus* through RNA interference (RNAi) according to our established transformation method (Li et al., 2003). Because *VCM1* and *VCM2* have high homology, the designed RNAi construct (Supplemental Figure 2A) could not effectively differentiate them and might have suppressed both *VCM1* and *VCM2*. More than 50 independent transgenic lines of the *VCM1* and *VCM2* downregulation (DR) were generated via RNAi. Examination of the DR transgenics identified different levels of *VCM1* and *VCM2* DR (Supplemental Figure 2B). Among them, the transgenic plants displayed remarkable phenotypic changes when both *VCM1* and *VCM2* were substantially downregulated. After screening the transgenics, two transgenic lines, DR4 and DR15, which displayed dramatic suppression of both *VCM1* and *VCM2* expression (Supplemental Figure 2B), were multiplied through micro-cutting propagation for further characterization. Meanwhile, we overexpressed *VCM1* in order to investigate the implications of its upregulation in *Populus*. More than 30 independent overexpression lines were generated. The transgenic plants showed various levels of *VCM1* expression. After the transgenic lines were screened for *VCM1* upregulation (UR), two lines, UR13 and UR25, displayed substantial upregulation of *VCM1* expression (Supplemental Figure 2C) and phenotypic changes. Thus, UR13 and UR25 were multiplied through micro-cutting propagation and used for characterization along with the DR transgenics.

The DR plants displayed significantly shorter internodes, while the UR plants showed longer internodes (Supplemental Figure 2D and 2G). The leaves of DR plants were smaller, softer, and darker green with smooth margins and shorter petioles compared with those of UR plants (Supplemental

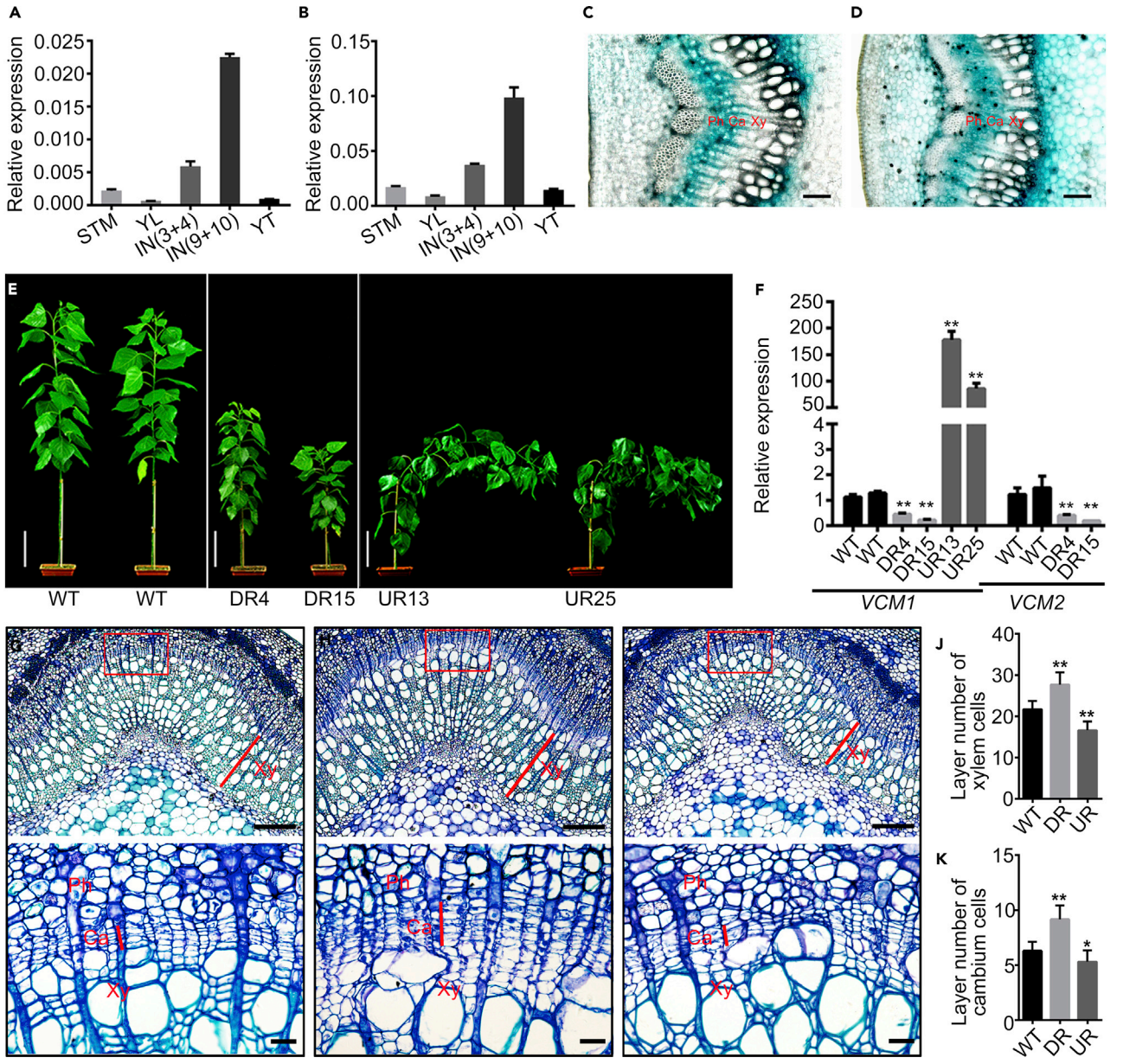

Figure 1. *VCM1* and *VCM2* expression and phenotypes of their transgenic lines.

(A and B) qRT-PCR analysis of *VCM1* **(A)** and *VCM2* **(B)** expression in different tissues. Values are means ± SD (n = 3 biological replicates). SMT, shoot meristem tissue; YL, young leaf; IN, internode; YT, young roots.

(C and D) GUS activity in transgenic *Populus* driven by the *VCM1* promoter **(C)** and the *VCM2* promoter **(D)**. Ca, cambium; Xy, xylem; Ph, phloem. Scale bar corresponds to 100 μm.

(E) Phenotypes of the wild-type (WT), *VCM1* and *VCM2* knock-down lines, (*DR4* and *DR15*) and *VCM1* overexpression lines (*UR13* and *UR25*). Scale bar corresponds to 10 cm.

(F) qRT-PCR analysis of *VCM1* and *VCM2* expression in transgenics. Values are means ± SD (n = 3 biological replicates).

(G–I) Cross-section of the 13th internode stained with toluidine blue (above) and enlarged rectangle area (below). **(G)** WT; **(H)** *VCM1* and *VCM2* knock-down lines; **(I)**, *VCM1* overexpression lines. Xy, xylem; Ph, phloem; Ca, cambium. Scale bars correspond to 200 μm (50 μm in enlargements).

(J) Number of cambium cell layers (n > 50).

(K) Number of xylem cell layers (n > 50). Plants used for analysis were grown in a phytotron for 3 months. Values are means ± SD. Statistical significance of differences was calculated based on two-tailed, two-sample Student's t-test (**P < 0.01, *P < 0.05).

Figure 2E and 2H). DR plants showed a dwarfed stature, while UR plants displayed a lodging stem phenotype when grown in a phytotron for 3 months (Figure 1E). The expression of *VCM1* and *VCM2* was stably downregulated or upregulated in these transgenics after multiple propagations (Figure 1F). In cross-sections, compared with the wild-type (WT) (Figure 1G), the downregulation of *VCM1* and *VCM2* expression resulted in more xylem tissue formation (Figure 1H), while the upregulation of *VCM1* expression inhibited xylem increment (Figure 1I). This is indicated by the cell layers generated in the cambium

dividing zone and secondary xylem tissue. In successive cell files, *VCM1* and *VCM2* DR plants showed more layers of cells in the cambium zone and secondary xylem tissue, while *VCM1* UR plants displayed fewer layers of cells produced in secondary growth (Figure 1J and 1K). After growth in a greenhouse for more than 5 months, the stem diameter of DR plants was greater compared with the WT, whereas that of UR plants was smaller (Supplemental Figure 2F and 2I). These results suggest that *VCM1* and *VCM2* negatively regulate vascular cambium proliferation activity and xylem tissue increment in *Populus*.

VCM1 regulates *PIN5b* expression

Next, we more closely investigated the processes by which *VCM* genes affect the secondary growth of *Populus*. VCM1 and VCM2 were detected to be localized in the nucleus (Supplemental Figure 3) as expected, consistent with their nature as transcription factors. We performed RNA sequencing of the tissue undergoing secondary growth in *VCM1* and *VCM2* DR plants and the transcriptomes of secondary growth tissues were substantially modified (Supplemental Figure 4A). Compared with WT plants, the top 10 enriched KEGG pathways of differentially expressed genes (DEGs) mainly included plant hormone signaling, mitogen-activated protein kinase signaling, and amino acid metabolism (Supplemental Figure 4B). Particularly, the most prominent changes occurred in genes related to auxin transport and response (Figure 2A and 2B). Given the correlation between auxin and secondary growth, the effect of *VCM1* and *VCM2* on stem growth could regulate auxin-related genes. Among these genes, *PIN5b* was substantially downregulated in *VCM1* and *VCM2* DR plants (Figure 2B). Further analysis confirmed that *PIN5b* expression was downregulated in DR15 and upregulated in UR13 plants (Figure 2C). However, the other *PIN* homologs either expressed at much lower levels or showed a discrete expression pattern (Supplemental Figure 4C). In addition, cells from various tissues in the stem were collected using a microdissection laser capture system for transcript analysis. *PIN5b*, *VCM1*, and *VCM2* showed similar expression profiles and tissue specificity in the vascular cambium area (Figure 3A).

To investigate whether *VCM1* directly regulates *PIN5* expression, we examined the binding of VCM1 to the *PIN5b* promoter. *VCM1* was fused with a FLAG tag and transferred into *Populus*. The expressed VCM1 protein was detected in the stem using a FLAG antibody (Figure 3B). Chromatin immunoprecipitation (ChIP) was then carried out to identify VCM1-bound DNA fragments. A ChIP-qPCR assay verified the binding of VCM1 to the fragments in the *PIN5b* promoter, which contained the predicted binding elements of MADS-boxes (Figure 3C and 3D). Together, these results indicate that *VCM1* regulates *PIN5* expression presumably by binding to its promoter.

VCM1 regulates cytosolic auxin levels across the vascular cambium area

We then investigated whether *VCM1* affects cytosolic IAA levels as *VCM1* expression regulates *PIN5b* expression. IAA can be detected by free IAA-specific antibodies in the cytosol (Shi et al., 1993; Avsian-Kretchmer et al., 2002; Marquez-Lopez et al., 2018). Using a specific antibody, we examined cytosolic IAA levels in the vascular cambium area of DR and UR transgenics. IAA levels were higher in DR plants but lower in UR plants compared with the WT (Figure 4A–4D). The difference in IAA levels detected by IAA-specific antibodies was further verified by IAA determination through chemical analysis. Compared with WT plants, the IAA content in the stem was significantly increased in DR plants but decreased in UP plants (Figure 4E). These analyses demonstrate that the modification of *VCM1* and *VCM2* expression alters cytosolic IAA levels across the vascular cambium area, which in turn regulates cambium proliferation activity and xylem differentiation in the process of secondary growth in *Populus*.

Overexpression of *PIN5b* represses cambium proliferation activity and modifies cytosolic auxin levels

Next, we overexpressed *PIN5b* in *Populus*. *PIN5b*-overexpression plants, POE5 and POE11, were multiply propagated and analyzed in detail. POE5 and POE11 transgenic plants displayed a smaller stature (Figure 5A) and significantly increased *PIN5b* expression compared with the control (Figure 5B). The stems of the transgenics developed narrower cambium regions with fewer layers of cell proliferation compared with WT plants (Figure 5C and 5D). We then analyzed the cytosolic IAA level *in vivo* through IAA immunolocalization (Figure 6). In WT plants, a gradient level of cytosolic IAA was detected in the cambium, developing phloem, and developing xylem (Figure 6B), by contrast, the IAA level was reduced in *PIN5b*-overexpression lines (Figure 6C). These results suggest that *PIN5b* reduces the cytosolic IAA level in the vascular cambium area in *Populus*.

DISCUSSION

In trees, the secondary growth of stem depends on cambium proliferation activity. During secondary growth, a concentration gradient of active auxin across the vascular cambium area provides hormone signals that regulate cambium activity and secondary xylem differentiation (Sundberg et al., 2000). In this study, we identified two MADS-box genes, *VCM1* and *VCM2*, in *Populus*, which are specifically expressed in association with secondary growth. Genetic evidence showed that *VCM1* and *VCM2* function redundantly in the regulation of vascular cambium activity and the formation of secondary xylem tissue. *VCM1* and *VCM2* likely regulate *PIN5b* expression across the vascular cambium area and tune the cytosolic IAA level through intracellular auxin transport. This study reveals the mechanism underlying the regulation of auxin concentration across the vascular cambium area, which is essential for the secondary growth of stem in trees (Figure 7).

VCM1 and *VCM2* regulate the secondary growth of stem in *Populus*

In plants, MADS-box genes encode a large family of transcription factors that play various roles in diverse developmental processes and in response to stress (Smaczniak et al., 2012; Castelan-Munoz et al., 2019). Although studies have shown the importance of MADS-box genes in regulatory networks, many members of this family are function-unknown. In *Populus*, 105 putative functional MADS-box genes have been identified in the tree genome (Leseberg et al., 2006). Few of them have known functions in the process of tree development.

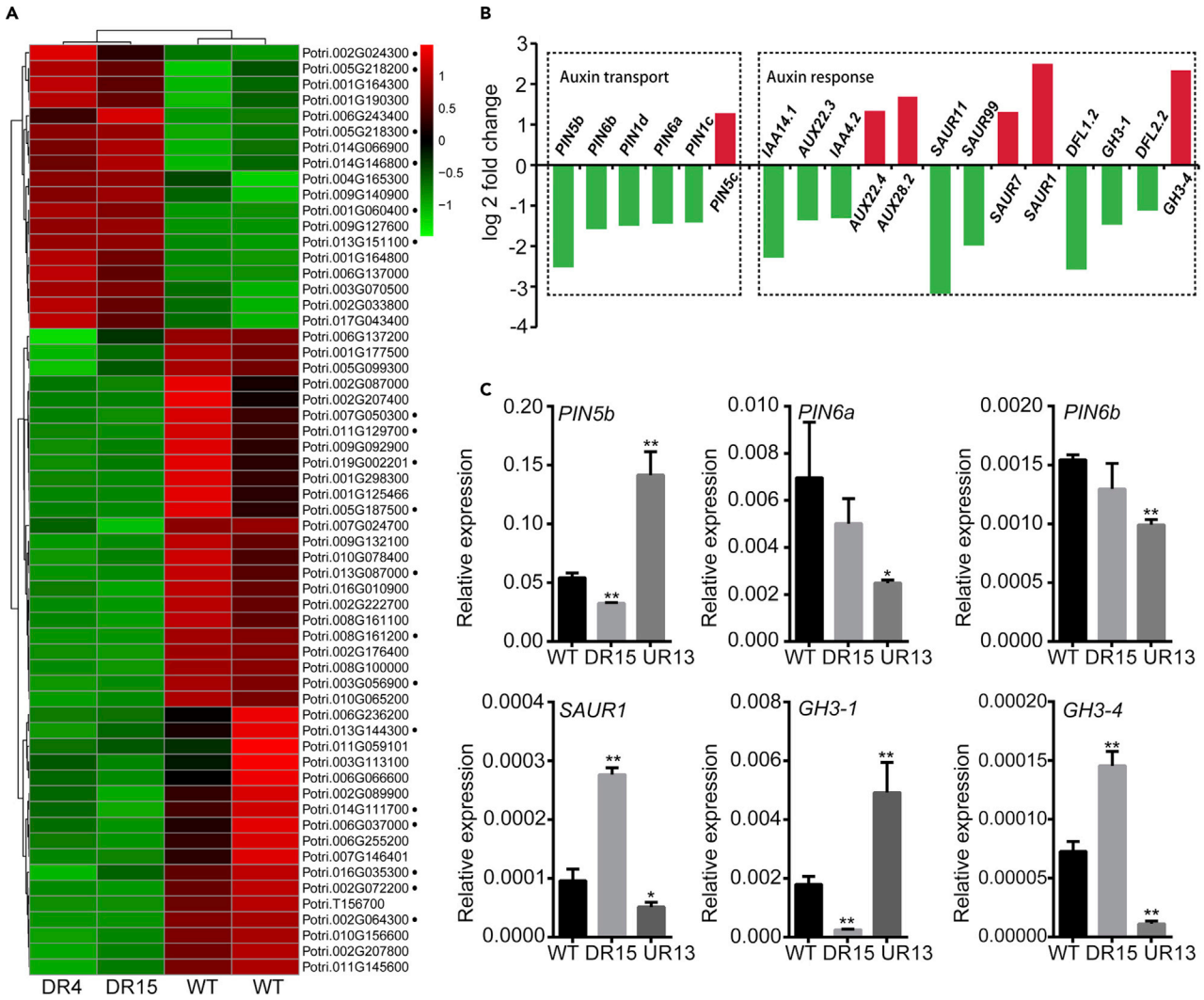

Figure 2. Expression of auxin-related genes upon the regulation of *VCM1* and *VCM2*.

(A) Heatmap of auxin-related gene expression in the transcriptomes of WT and *VCM1* and *VCM2* knock-down plants.

(B) Log2 value of differentially expressed auxin transport and responsive genes.

(C) qRT-PCR analysis of the expression of auxin-related genes. Values are means ± SD ($n = 3$ biological replicates). Statistical significance of differences was calculated based on two-tailed, two-sample Student's *t*-test (**$P < 0.01$,*$P < 0.05$).

Perennial trees feature the secondary growth of stem that depends on vascular cambium proliferation activity. When we analyzed the development of the vascular cambium, we found that the expression of two function-unknown MADS-box genes, *VCM1* and *VCM2*, were modified when the vascular cambium became defective. *VCM1* and *VCM2* are highly homologous genes in *Populus*. Interestingly, when the *VCM1* or *VCM2* sequence was used to BLAST GenBank, matching homologs with high similarity were found primarily in woody plant species. This may indicate a link between the function of *VCM1* and *VCM2* and woody plant development. Meanwhile, *VCM1* and *VCM2* were preferentially expressed in tissues undergoing secondary growth. Simultaneous suppression of *VCM1* and *VCM2* promoted vascular cambium proliferation activity and enhanced the secondary growth of stem. These observations suggest that *VCM1* and *VCM2* negatively regulate secondary growth in a redundant manner in *Populus*.

In *Populus*, secondary growth is perennially maintained, and the underlying regulatory system is presumably different from that of annual plants. The involvement of *VCM1* and *VCM2* in *Populus* secondary growth helps to understand how secondary growth is regulated in trees and why it continues over a long period.

PIN5b modulates auxin homeostasis in the vascular cambium area during secondary growth in *Populus*

Studies have indicated that auxin is involved in vascular tissue formation (Mattsson et al., 1999; Sieburth, 1999; De Rybel et al., 2014). The local maximum concentration of auxin in cells with xylem identity in *Arabidopsis* root cambium modulates cambium activity and the differentiation of vascular tissues (Smetana et al., 2019). In trees, auxin plays a critical role in the secondary growth of stem (Uggla et al., 1996). Across the vascular cambium area, the auxin concentration shows a gradient distribution (Uggla et al., 1996, 1998). Directional cell-to-cell

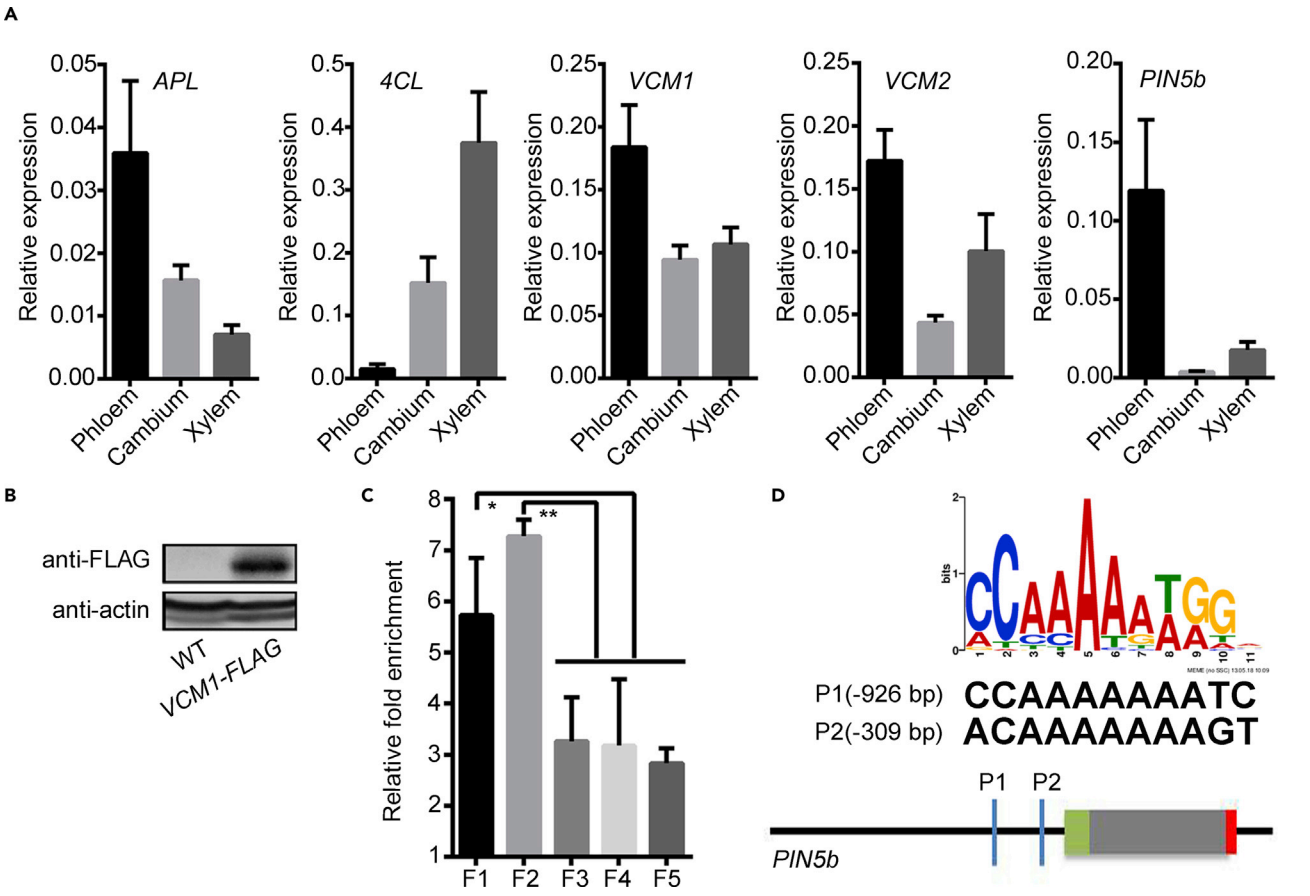

Figure 3. Expression of *VCM1, VCM2*, and *PIN5b* in cells undergoing secondary growth and the binding of VCM1 to *PIN5b* promoter.

(A) Cells were collected from the phloem, cambium, and xylem using a microdissection laser capture system. The expression of *VCM1*, *VCM2*, and *PIN5b* in cells was measured by qRT-PCR analysis. *APL* was used as a reference for phloem-preferred expression and *4CL1* as a reference for xylem-preferred expression.

(B) VCM1 was detected in the transgenics expressing *VCM1-FLAG* and used for ChIP analysis.

(C) Five fragments from the *PIN5b* promoter and intron (F1: −1209 to −899; F2: −451 to − 188; F3: −1815 to −1519; F4: +1724 to +1856; F5: +1930 to +2123) were examined for enrichment in VCM1-binding precipitation.

(D) Fragments F1 and F2 in the *PIN5b* promoter region contain possible binding elements P1 and P2, respectively. Values are means ± SD ($n = 3$ biological replicates). Statistical significance of differences was calculated based on two-tailed, two-sample Student's *t*-test (**$P < 0.01$, *$P < 0.05$).

auxin transport and intracellular auxin compartmentation are two major means of auxin translocation (Park et al., 2017). It is unclear how auxin concentration is regulated, especially in the cambium area, and how local auxin concentration affects the secondary growth of stem. The cellular auxin concentration is regulated by auxin biosynthesis, metabolism, and movement (Park et al., 2017). In this study, we found that intracellular auxin transport plays a role in tuning cellular auxin concentration across the vascular cambium area.

Detection of auxin via immunolocalization at the cellular level has been a useful tool for visualizing free IAA signals in a number of species (Avsian-Kretchmer et al., 2002; Forestan and Varotto, 2013; Marquez-Lopez et al., 2018; Yan et al., 2020). Using specific anti-IAA monoclonal antibodies, we performed IAA immunolocalization in *Populus*, which allowed us to detect the cellular free IAA level in the cambium, phloem, and developing xylem cells. The results are in good agreement with those obtained by IAA chemical analysis in stem tissues. The overexpression of *PIN5b* reduced the cytosolic IAA level, presumably through the transporter activity of PIN5b to relocate IAA from the cytosol to the ER lumen. These results reveal that the cellular IAA concentration across the vascular cambium area is tuned by intracellular transport mediated by PIN5b. Because the output of auxin signaling is mainly determined by cytosolic IAA levels (Dharmasiri et al., 2005; Kepinski and Leyser, 2005), intracellular IAA transport may regulate cytosolic auxin concentration, which serves as a signal that modulates secondary growth in trees.

PIN5 transporters are suggested to be localized in the ER, and the subcellular homeostasis of auxin is modulated by the transport of auxin from the cytosol to the ER lumen (Mravec et al., 2009; Ding et al., 2012). *Populus PIN5* homologs are preferentially expressed across the area of the vascular cambium and localized in the ER (Liu et al., 2014). A *PIN5* homolog has been reported to regulate cellular auxin levels in *Populus* (Johnsson et al., 2019). In our study, the expression of *PIN5b* was activated by *VCM1* and *VCM2* in relation to secondary growth. *PIN5b* overexpression reduced cambium activity and inhibited secondary growth. This

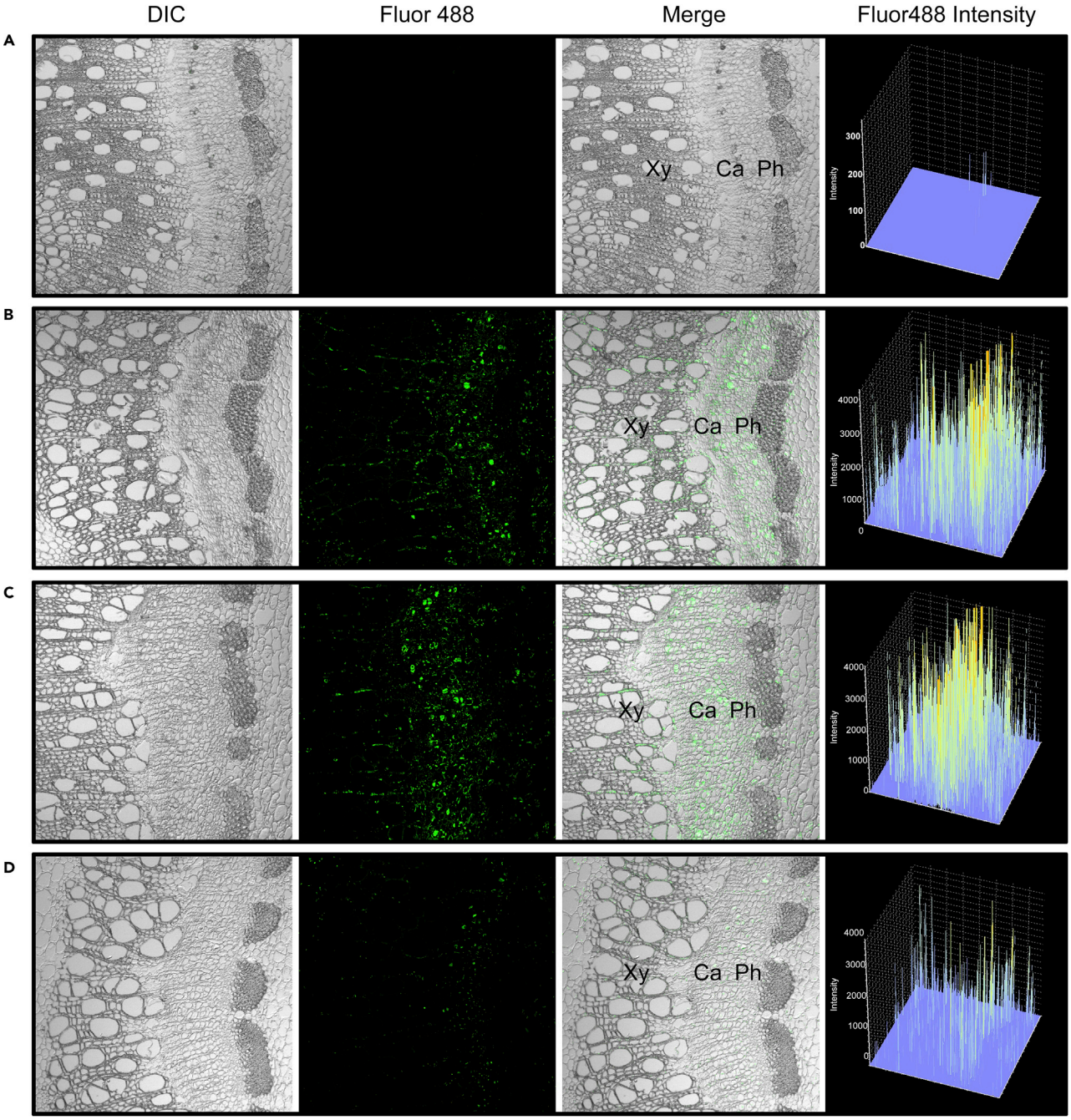

E

Sample	IAA	IAA-Asp	IAA-Leu	IAA-Ala	IAA-Glu
WT	1.636 ± 0.058	0.027 ± 0.003	0.043 ± 0.006	n.d.	n.d.
DR	2.065 ± 0.038	0.047 ± 0.002	0.042 ± 0.006	n.d.	n.d.
UR	0.641 ± 0.028	0.023 ± 0.003	0.029 ± 0.003	n.d.	n.d.
	$p < 0.01$	$p < 0.01$	$p < 0.05$		

Values are means ± SD; Unit: ng.cm^{-1} F.W.; n.d., not detected.

(legend on next page)

suggests that the tuning of cellular auxin level by *PIN5b* regulates secondary growth in *Populus*.

VCM1 and *VCM2* regulate secondary growth through PIN5b function in intracellular IAA transport

In trees, the secondary growth of stem gives rise to wood formation, and sophisticated transcriptional networks are involved in controlling vascular cambium division and descendant xylem cell differentiation (Demura and Fukuda, 2007; Zhang et al., 2014). A great deal of interest has been invested to identify and construct the hierarchical transcriptional networks involved in the regulation of vascular cambium activity, cell proliferation, xylem differentiation, and cell wall thickening using both *Arabidopsis* and *Populus* systems (Hertzberg et al., 2001; Ko et al., 2004; Andersson-Gunneras et al., 2006; Zhang et al., 2019). Although progress has been made in revealing how secondary growth is regulated through transcriptional networks, more studies are needed to fully understand the mechanism of secondary growth. Here, two function-unknown MADS-box transcription factor genes, *VCM1* and *VCM2*, were found to be involved in the regulation of vascular cambium activity and subsequent wood formation in *Populus*. The downregulation of *VCM1* and *VCM2* expression resulted in an increase of vascular cambium proliferation activity and wood formation, whereas in the cells of the vascular cambium area, the regulation of *VCM1* and *VCM2* expression affected cytosolic IAA level and auxin signaling. *VCM1*/*VCM2* and *PIN5b* displayed the same specificity of expression in the vascular cambium area. Evidence also suggested that *VCM1* binds to the *PIN5* promoter and regulates its expression. Thus, *VCM1*/*VCM2* and *PIN5b* may act in a regulatory pathway to tune the level of cytosolic IAA in vascular cambium cells, which in turn serves as a hormone signal to modulate the secondary growth of stem (Figure 7).

Although an IAA concentration gradient is known to exist across the vascular cambium area, more insights into the regulation and establishment of IAA signaling are essential, given its effects on vascular cambium activity, cell proliferation, and xylem differentiation. Our study reveals a transcription regulatory pathway behind the observed phenomenon and an explanation for a better mechanistic understanding of the secondary growth of stem.

MATERIAL AND METHODS

Plant material and growth conditions

The *Populus* tree (*Populus deltoides* × *P. euramericana* cv. Nanlin895) used in this study was grown in a phytotron with a light/dark cycle of 14/10 h under 60% relative humidity at 25°C.

Gene sequence analysis

The amino acid sequences of VCM1 and VCM2 were obtained from the *Populus* genome database (www.phytozome.net/poplar). *VCM1* and *VCM2* homologs were searched in the NCBI database using BLAST and aligned using CLUSTALW. The phylogenetic relationship was analyzed in MEGA 6.0 (Tamura et al., 2013) using the neighbor-joining method. Bootstrap values were calculated from 1000 trials. Full-length *VCM1* and *VCM2* coding sequences were cloned from the *Populus* clone Nanlin895.

Gene expression analysis

Total RNA was isolated from SMT, leaves, different stem internodes, and roots using a total RNA kit following the manufacturer's instructions (Omega, R6827-02). The first-strand cDNA was synthesized from total RNA using cDNA Synthesis SuperMix (TransGen, AT311-03) and used for the qRT-PCR analysis of gene expression using gene-specific primers (Supplemental Table 2). qRT-PCR was performed using PerfectStart Green qPCR SuperMix (TransGen, AQ601) and a QuantStudio 3 Real-Time PCR Detection System (Thermo Fisher Scientific) according to the manufacturer's instructions. For the normalization of target gene expression in each sample, *Actin2* (Potri.001G309500) was used as an internal control.

Constructs and transformation

Nanlin895 was used for genetic transformation according to the protocol used in our lab (Li et al., 2003). For promoter analysis, ~2.5 kb fragments from *VCM1* and *VCM2* promoters were cloned from *Populus*, respectively. The promoter fragment was cloned into a *pCAMBIA2300-GUS* vector upstream of uidA (*GUS*) and transferred to *Populus* for GUS activity analysis. For the downregulation of *VCM*, a fragment (245 bp) of *VCM2* was constructed to form a hairpin structure that would function as an RNAi suppressor under the control of the CaMV 35S promoter. Because *VCM1* and *VCM2* share high homology, the RNAi construct may target both of them when it is transferred to *Populus* for the generation of knock-down lines. Meanwhile, for upregulation, *VCM1* was transferred to *Populus* under the control of the CaMV 35S promoter. On the other hand, the full coding region of *PIN5b* was subcloned into vector *pCAMBIA2300* under the control of the CaMV 35S promoter and transferred to *Populus*. *Agrobacterium* strain GV3101 was used for mediating *Populus* transformation. To determine the subcellular localization of VCM proteins, YFP-VCM1 and YFP-VCM2 fusion proteins were constructed under the control of the CaMV 35S promoter and introduced into tobacco leaves through *Agrobacterium*-mediated transformation. Primers used for vector construction are listed in Supplemental Table 2.

Histochemical staining

For GUS staining, convenient cross-sections of the stem were incubated in 50% acetone (v/v) for 10 min on ice and then stained in GUS solution (100 mM sodium phosphate [pH 7.0], 10 mM EDTA, 0.5 mM ferrocyanide, 0.1% Triton X-100, 20% methanol, and 2 mM X-Gluc) at 37°C. After staining, sections were cleared by 70% ethanol, washed using ddH_2O, cleared by chloral hydrate (7.5% [w/v] gum arabic, 6.05 M chloral hydrate, and 5% glycerol [v/v]), and photographed. For the analysis of stem structure, stem internodes were fixed, paraffin-embedded, sectioned, and observed as described previously (Zhu et al., 2018)

RNA sequencing

Total RNA was isolated from stem internodes using a total RNA kit according to the manufacturer's instructions (Omega, R6827-02) after a combination of three biological repeats of independent lines of the transgenic and WT plants. After the RNA quality was confirmed, 5 μg of the total RNA was used to construct a cDNA library using the TruSeq Stranded mRNA LT Sample Prep Kit (Illumina, RS-122-2101) and Agencourt

Figure 4. Detection of cytosolic IAA in the regulation of *VCM1*and *VCM2*.
(A–D) Cytosolic IAA was detected through immune-histochemical fluorescence analysis using IAA-specific antibodies and the fluorescence signal in the examined area is quantified as intensity. IgG served as the negative control. **(A)** WT; **(B)** *VCM1* and *VCM2* knock-down plants; **(C)** *VCM1* overexpression plants; **(D)** Ca, cambium; Xy, xylem; Ph, phloem.
(E) Chemical determination of IAA and its amino acid conjugates. Values are means ± SD (n = 3 biological replicates). Tissues from the 10th to 14th internodes were collected for analysis. Statistical significance of differences was calculated based on two-tailed, two-sample Student's t-test.

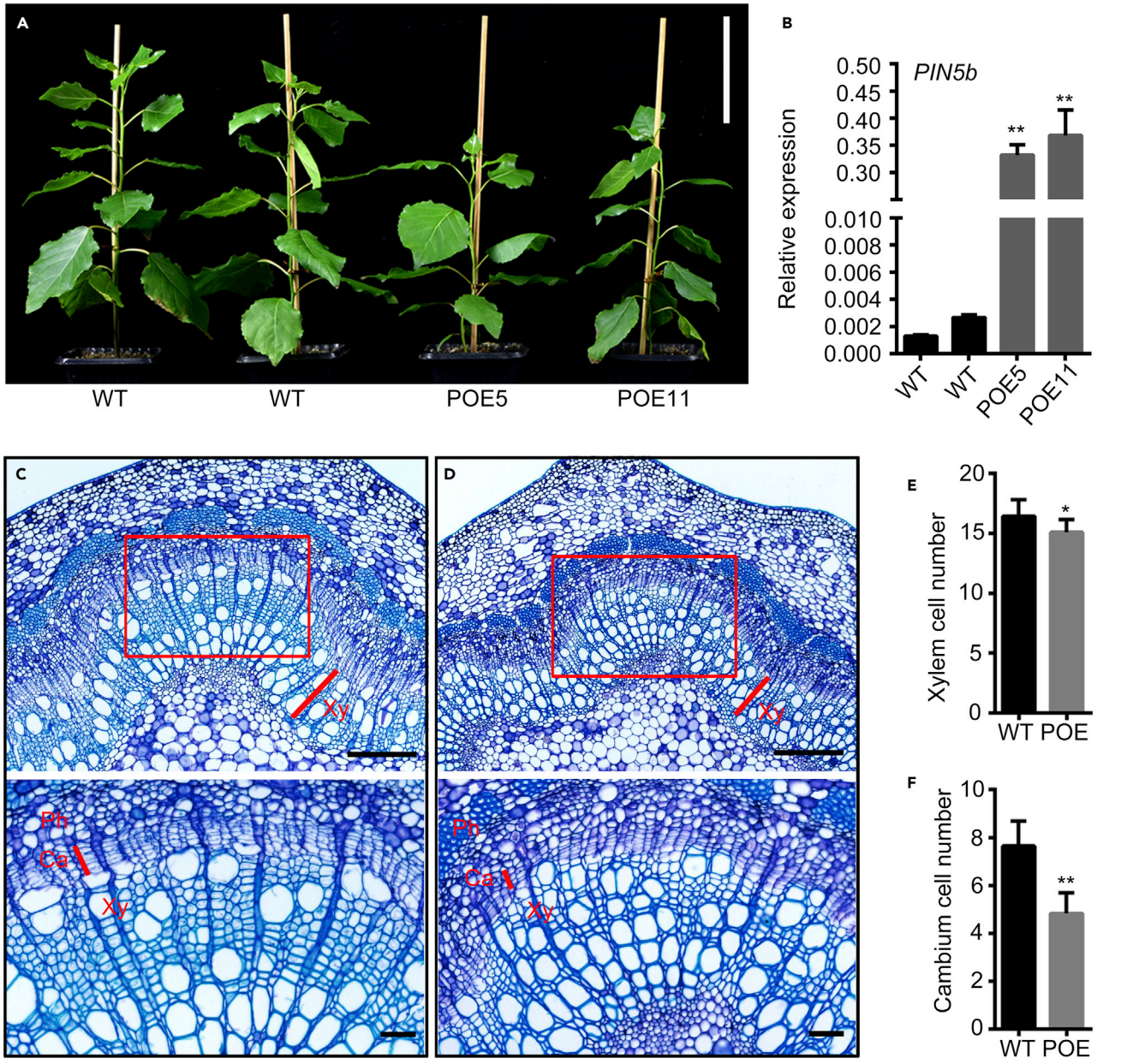

Figure 5. Phenotypes of *PIN5b* overexpression lines.

(A) WT and *PIN5b* overexpression lines (POE5 and POE11) were grown in a phytotron for 2 months. Scale bar corresponds to 9 cm.

(B) *PIN5b* expression. Values are means ± SD (n = 3 biological replicates).

(C and D) Cross-section of the 11th internode stained with toluidine blue (above) and enlarged rectangle area (below). **(C)** WT; **(D)** *PIN5b* overexpression lines. Xy, xylem; Ph, phloem; Ca, cambium. Scale bars correspond to 200 μm (50 μm in enlargements).

(E) Number of xylem cell layers (n > 50).

(F) Number of cambium cell layers (n > 50). Values are means ± SD. Statistical significance of differences was calculated based on two-tailed, two-sample Student's t-test (**P < 0.01, *P < 0.05).

AMPure XP (Beckman Coulter, A63881). The cDNA library was quality controlled using the Agilent 2100 Bioanalyzer and sequenced using the 150 bp paired-end sequencing strategy, which was performed on the Illumina HiSeq X10 platform. Raw data (raw reads) were processed using the NGS QC Toolkit (Patel and Jain, 2012). Clean reads were mapped to the genome of *Populus trichocarpa* (http://phytozome.jgi.doe.gov/) using the HISAT2 program with default parameters (Kim et al., 2015). Fragments per kilobase per million were calculated using Cufflinks (Roberts et al., 2011). DEGs were identified using the DESeq R package with the estimateSizeFactors and nbinomTest functions. P < 0.05 and fold change >2 or fold change <0.5 were set as the threshold for significantly differential expression. KEGG pathway enrichment analysis of DEGs was performed using R based on the hypergeometric distribution (Kanehisa et al., 2008).

Laser microdissection

Internodes (8th–10th) from WT plants were sampled for stem sectioning. Laser microdissection, RNA extraction, RNA amplification, and qRT-PCR

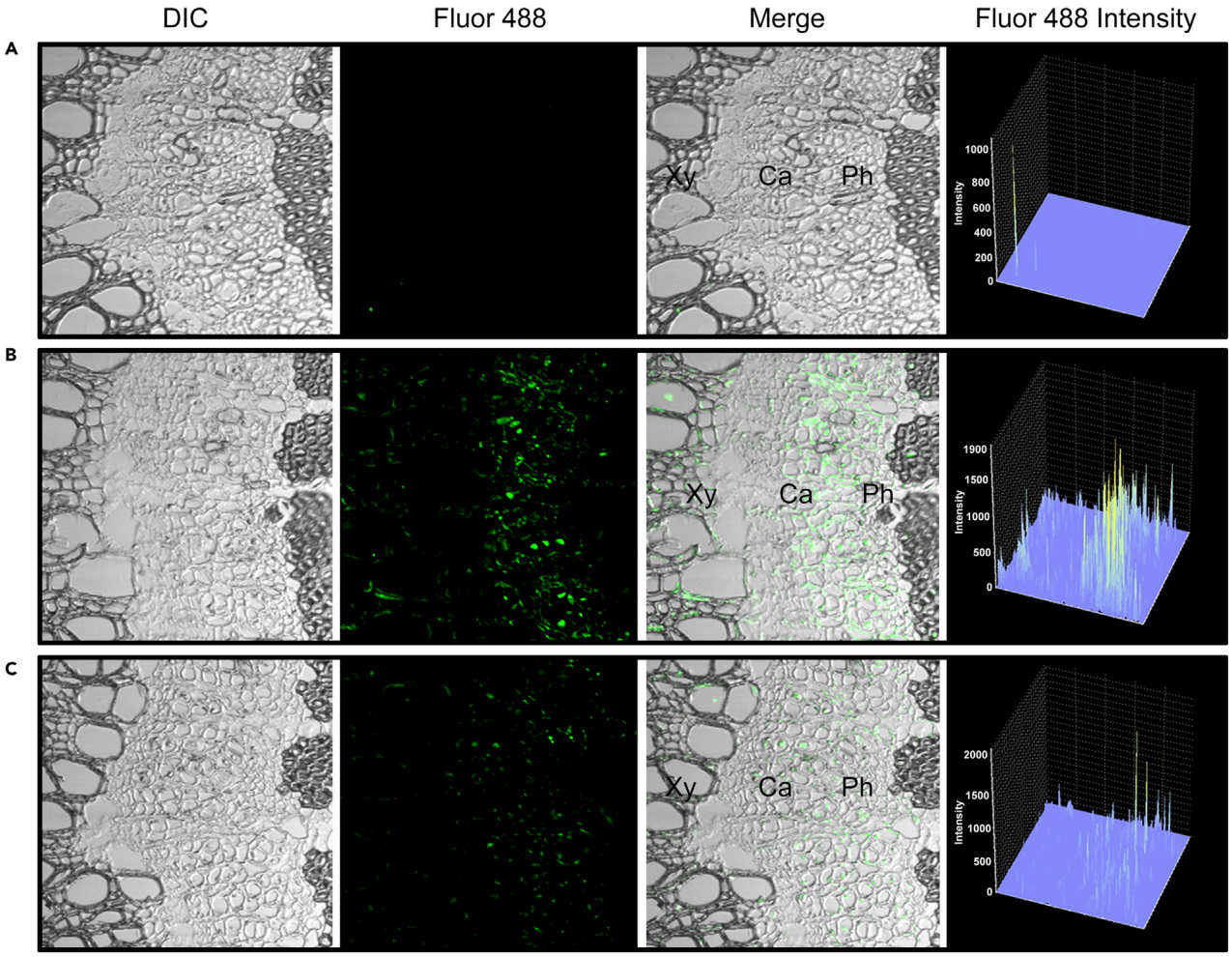

Figure 6. Detection of cytosolic IAA in the *PIN5b* overexpression line.
(A–C) Cytosolic IAA was detected using IAA-specific antibodies and the fluorescence signal in the examined area was quantified as intensity. **(A)** Negative control IgG; **(B)** WT; **(C)** *PIN5b* overexpression line. Ca, cambium; Xy, xylem; Ph, phloem.

measurement were conducted as described previously (Song et al., 2010). Primers used for PCR analysis are listed in Supplemental Table 2.

ChIP

For the ChIP analysis, stem internodes were sampled from WT and transgenic plants. The transgenics expressing VCM1-FLAG were used to isolate proteins for western blot analysis using an anti-FLAG antibody (Abmart, M2008L). ChIP was performed as described previously (Bowler et al., 2004) using a Magna ChIP A/G Kit (Millipore). The bound DNA fragments were analyzed using qRT-PCR. The primers are listed in Supplemental Table 2.

IAA immunolocalization and analysis

Based on the previously described method of IAA immunolocalization (Marquez-Lopez et al., 2018), a modification was made for IAA detection in the *Populus* stem tissue. In brief, stem segments (3 mm in length) from transgenic and WT *Populus* were prefixed in 3% EDAC (1-Ethyl-3-(3-Dimethylaminopropyl)Carbodiimide Hydrochloride) (ABCONE) in 1× PBS (137 mM NaCl, 2.7 mM KCl, 10 mM Na_2HPO_4, 2 mM KH_2PO_4 [pH 7.4]). To remove the gas from stem tissues, vacuum was applied two to three times to ensure that the stem was completely submerged in the solution. The stem tissues were then stored at 4°C for 30 min. After the samples were fixed in a formaldehyde-acetic acid solution (formaldehyde:glacial acetic acid:70% ethanol [1:1:18]) for 24–48 h, they were dehydrated via a graded ethanol series and embedded in paraffin. The stem samples were sectioned to a thickness of 10 μm using a rotary microtome (Leica RM2235). Sections were incubated with an IAA-specific antibody (Sigma, A0855). Detection was carried out using Alexa Fluor 488 antibody (Abcam, ab150113) following a standard method. For the chemical determination of IAA, fresh internode tissues (from the 10th to the 14th stem internodes) were ground to a fine powder in liquid nitrogen, and 0.5 g of sample was used for the determination of IAA and its amino acid conjugates according to a previously reported method (Matsuda et al., 2005).

ACCESSION NUMBERS

NCBI GenBank accession numbers: *VCM1*, XM024582264.1; *VCM2*, XM002321675.3; and *PIN5b*, XM006375996.2.

SUPPLEMENTAL INFORMATION

Supplemental information is available at *Plant Communications Online*.

FUNDING

This work was supported by the Ministry of Science and Technology of the People's Republic of China (2016YFD0600104), the National Natural

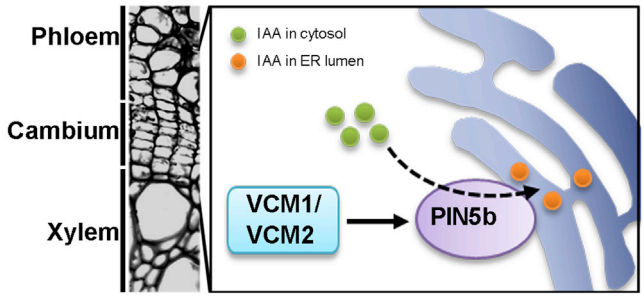

Figure 7. A proposed model for the involvement of *VCM1* and *VCM2* in regulating secondary growth.
VCM1 and *VCM2* regulate *PIN5b* expression in the cambium area. PIN5b transports IAA from the cytosol to the ER lumen, thereby tuning the cytosolic IAA concentration. Thus, *VCM1* and *VCM2* play a critical role in regulating vascular cambium proliferation and secondary growth through modulating auxin homeostasis.

Science Foundation of China(31630014), and the Strategic Priority Research Program of the Chinese Academy of Sciences (XDB27020104).

AUTHOR CONTRIBUTIONS

S.Z., J.S., and L.L. conceived the experiments. S.Z., J.H., Z.L., Y.Z., and J.S. performed the experiments. S.Z. and L.L. analyzed the data and wrote the manuscript.

ACKNOWLEDGMENTS

We thank Shuining Yin for her support in fluorescence microscopy and Xiaoli Liu for assistance with ChIP experiments. No conflict of interest declared.

Received: August 22, 2020
Revised: November 2, 2020
Accepted: November 19, 2020
Published: November 23, 2020

REFERENCES

Andersson-Gunneras, S., Mellerowicz, E.J., Love, J., Segerman, B., Ohmiya, Y., Coutinho, P.M., Nilsson, P., Henrissat, B., Moritz, T., and Sundberg, B. (2006). Biosynthesis of cellulose-enriched tension wood in *Populus*: global analysis of transcripts and metabolites identifies biochemical and developmental regulators in secondary wall biosynthesis. Plant J. **45**:144–165.

Arora, R., Agarwal, P., Ray, S., Singh, A.K., Singh, V.P., Tyagi, A.K., and Kapoor, S. (2007). MADS-box gene family in rice: genome-wide identification, organization and expression profiling during reproductive development and stress. BMC Genomics **8**:242.

Avsian-Kretchmer, O., Cheng, J.C., Chen, L.J., Moctezuma, E., and Sung, Z.R. (2002). Indole acetic acid distribution coincides with vascular differentiation pattern during *Arabidopsis* leaf ontogeny. Plant Physiol. **130**:199–209.

Baba, K., Karlberg, A., Schmidt, J., Schrader, J., Hvidsten, T.R., Bako, L., and Bhalerao, R.P. (2011). Activity-dormancy transition in the cambial meristem involves stage-specific modulation of auxin response in hybrid aspen. Proc. Natl. Acad. Sci. U S A **108**:3418–3423.

Bjorklund, S., Antti, H., Uddestrand, I., Moritz, T., and Sundberg, B. (2007). Cross-talk between gibberellin and auxin in development of *Populus* wood: gibberellin stimulates polar auxin transport and has a common transcriptome with auxin. Plant J. **52**:499–511.

Campbell, L., and Turner, S. (2017). Regulation of vascular cell division. J. Exp. Bot. **68**:27–43.

Castelan-Munoz, N., Herrera, J., Cajero-Sanchez, W., Arrizubieta, M., Trejo, C., Garcia-Ponce, B., Sanchez, M.D., Alvarez-Buylla, E.R., and Garay-Arroyo, A. (2019). MADS-box genes are key components of genetic regulatory networks involved in abiotic stress and plastic developmental responses in plants. Front. Plant Sci. **10**:853.

De Rybel, B., Adibi, M., Breda, A.S., Wendrich, J.R., Smit, M.E., Novak, O., Yamaguchi, N., Yoshida, S., Van Isterdael, G., Palovaara, J., et al. (2014). Plant development. Integration of growth and patterning during vascular tissue formation in *Arabidopsis*. Science **345**:1255215.

Demura, T., and Fukuda, H. (2007). Transcriptional regulation in wood formation. Trends Plant Sci. **12**:64–70.

Dharmasiri, N., Dharmasiri, S., and Estelle, M. (2005). The F-box protein TIR1 is an auxin receptor. Nature **435**:441–445.

Ding, Z.J., Wang, B.J., Moreno, I., Duplakova, N., Simon, S., Carraro, N., Reemmer, J., Pencik, A., Chen, X., Tejos, R., et al. (2012). ER-localized auxin transporter PIN8 regulates auxin homeostasis and male gametophyte development in *Arabidopsis*. Nat. Commun. **3**:941.

Dornelas, M.C., Patreze, C.M., Angenent, G.C., and Immink, R.G.H. (2011). MADS: the missing link between identity and growth? Trends Plant Sci. **16**:89–97.

Fischer, U., Kucukoglu, M., Helariutta, Y., and Bhalerao, R.P. (2019). The dynamics of cambial stem cell activity. Annu. Rev. Plant Biol. **70 70**:293–319.

Forestan, C., and Varotto, S. (2013). Auxin immunolocalization in plant tissues. Methods Mol. Biol. **959**:223–233.

Gramzow, L., and Theissen, G. (2010). A hitchhiker's guide to the MADS world of plants. Genome Biol. **11**:214.

Grones, P., and Friml, J. (2015). Auxin transporters and binding proteins at a glance. J. Cell Sci. **128**:1–7.

Hertzberg, M., Aspeborg, H., Schrader, J., Andersson, A., Erlandsson, R., Blomqvist, K., Bhalerao, R., Uhlen, M., Teeri, T.T., Lundeberg, J., et al. (2001). A transcriptional roadmap to wood formation. Proc. Natl. Acad. Sci. U S A **98**:14732–14737.

Johnsson, C., Jin, X., Xue, W.Y., Dubreuil, C., Lezhneva, L., and Fischer, U. (2019). The plant hormone auxin directs timing of xylem development by inhibition of secondary cell wall deposition through repression of secondary wall NAC-domain transcription factors. Physiol. Plant. **165**:673–689.

Kanehisa, M., Araki, M., Goto, S., Hattori, M., Hirakawa, M., Itoh, M., Katayama, T., Kawashima, S., Okuda, S., Tokimatsu, T., et al. (2008). KEGG for linking genomes to life and the environment. Nucleic Acids Res. **36**:D480–D484.

Kepinski, S., and Leyser, O. (2005). The *Arabidopsis* F-box protein TIR1 is an auxin receptor. Nature **435**:446–451.

Kim, D., Landmead, B., and Salzberg, S.L. (2015). HISAT: a fast spliced aligner with low memory requirements. Nat. Methods **12**:357–U121.

Ko, J.H., Han, K.H., Park, S., and Yang, J.M. (2004). Plant body weight-induced secondary growth in *Arabidopsis* and its transcription phenotype revealed by whole-transcriptome profiling. Plant Physiol. **135**:1069–1083.

Leseberg, C.H., Li, A.L., Kang, H., Duvall, M., and Mao, L. (2006). Genome-wide analysis of the MADS-box gene family in *Populus trichocarpa*. Gene **378**:84–94.

Li, L., Zhou, Y.H., Cheng, X.F., Sun, J.Y., Marita, J.M., Ralph, J., and Chiang, V.L. (2003). Combinatorial modification of multiple lignin traits in trees through multigene cotransformation. Proc. Natl. Acad. Sci. U S A **100**:4939–4944.

Liu, B.B., Zhang, J., Wang, L., Li, J.B., Zheng, H.Q., Chen, J., and Lu, M.Z. (2014). A survey of *Populus* PIN-FORMED family genes reveals their diversified expression patterns. J. Exp. Bot. **65**:2437–2448.

Marquez-Lopez, R.E., Ku-Gonzalez, A., Mendez-Hernandez, H.A., Galaz-Avalos, R.M., and Loyola-Vargas, V.M. (2018). Auxin immunolocalization in *Coffea canephora* tissues. Methods Mol. Biol. **1815**:179–188.

Matsuda, F., Miyazawa, H., Wakasa, K., and Miyagawa, H. (2005). Quantification of indole-3-acetic acid and amino acid coniugates in rice by liquid chromatography-electrospray ionization-tandem mass spectrometry. Biosci. Biotechnol. Biochem. **69**:778–783.

Mattsson, J., Sung, Z.R., and Berleth, T. (1999). Responses of plant vascular systems to auxin transport inhibition. Development **126**:2979–2991.

Moyle, R., Schrader, J., Stenberg, A., Olsson, O., Saxena, S., Sandberg, G., and Bhalerao, R.P. (2002). Environmental and auxin regulation of wood formation involves members of the Aux/IAA gene family in hybrid aspen. Plant J. **31**:675–685.

Mravec, J., Skupa, P., Bailly, A., Hoyerova, K., Krecek, P., Bielach, A., Petrasek, J., Zhang, J., Gaykova, V., Stierhof, Y.D., et al. (2009). Subcellular homeostasis of phytohormone auxin is mediated by the ER-localized PIN5 transporter. Nature **459**:1136–U1127.

Nilsson, J., Karlberg, A., Antti, H., Lopez-Vernaza, M., Mellerowicz, E., Perrot-Rechenmann, C., Sandberg, G., and Bhalerao, R.P. (2008). Dissecting the molecular basis of the regulation of wood formation by auxin in hybrid aspen. Plant Cell **20**:843–855.

Parenicova, L., de Folter, S., Kieffer, M., Horner, D.S., Favalli, C., Busscher, J., Cook, H.E., Ingram, R.M., Kater, M.M., Davies, B., et al. (2003). Molecular and phylogenetic analyses of the complete MADS-box transcription factor family in *Arabidopsis*: new openings to the MADS world. Plant Cell **15**:1538–1551.

Park, J., Lee, Y., Martinoia, E., and Geisler, M. (2017). Plant hormone transporters: what we know and what we would like to know. BMC Biol. **15**:93.

Patel, R.K., and Jain, M. (2012). NGS QC Toolkit: a toolkit for quality control of next generation sequencing data. PLoS One **7**:e30619.

Petrasek, J., Mravec, J., Bouchard, R., Blakeslee, J.J., Abas, M., Seifertova, D., Wisniewska, J., Tadele, Z., Kubes, M., Covanova, M., et al. (2006). PIN proteins perform a rate-limiting function in cellular auxin efflux. Science **312**:914–918.

Roberts, A., Trapnell, C., Donaghey, J., Rinn, J.L., and Pachter, L. (2011). Improving RNA-Seq expression estimates by correcting for fragment bias. Genome Biol. **12**:R22.

Schrader, J., Moyle, R., Bhalerao, R., Hertzberg, M., Lundeberg, J., Nilsson, P., and Bhalerao, R.P. (2004). Cambial meristem dormancy in trees involves extensive remodelling of the transcriptome. Plant J. **40**:173–187.

Shi, L., Miller, I., and Moore, R. (1993). Immunocytochemical localization of indole-3-acetic-acid in primary roots of *Zea mays*. Plant Cell Environ. **16**:967–973.

Sieburth, L.E. (1999). Auxin is required for leaf vein pattern in *Arabidopsis*. Plant Physiol. **121**:1179–1190.

Smaczniak, C., Immink, R.G.H., Muino, J.M., Blanvillain, R., Busscher, M., Busscher-Lange, J., Dinh, Q.D., Liu, S.J., Westphal, A.H., Boeren, S., et al. (2012). Characterization of MADS-domain transcription factor complexes in *Arabidopsis* flower development. Proc. Natl. Acad. Sci. U S A **109**:1560–1565.

Smetana, O., Makila, R., Lyu, M., Amiryousefi, A., Rodriguez, F.S., Wu, M.F., Sole-Gil, A., Gavarron, M.L., Siligato, R., Miyashima, S., et al. (2019). High levels of auxin signalling define the stem-cell organizer of the vascular cambium. Nature **565**:485.

Song, Dongliang, Shen; Li (2010). Characterization of cellulose synthase complexes in Populus xylem differentiation. New Phytologist **187**:777–790.

Spicer, R., and Groover, A. (2010). Evolution of development of vascular cambia and secondary growth. New Phytol. **186**:577–592.

Sundberg, B., Uggla, C., and Tuominen, H. (2000). Cambial growth and auxin gradients. Cell Mol. Biol. Wood Form. 169–188.

Tamura, K., Stecher, G., Peterson, D., Filipski, A., and Kumar, S. (2013). MEGA6: molecular evolutionary genetics analysis version 6.0. Mol. Biol. Evol. **30**:2725–2729.

Tuominen, H., Puech, L., Fink, S., and Sundberg, B. (1997). A radial concentration gradient of indole-3-acetic acid is related to secondary xylem development in hybrid aspen. Plant Physiol. **115**:577–585.

Uggla, C., Mellerowicz, E.J., and Sundberg, B. (1998). Indole-3-acetic acid controls cambial growth in Scots pine by positional signaling. Plant Physiol. **117**:113–121.

Uggla, C., Moritz, T., Sandberg, G., and Sundberg, B. (1996). Auxin as a positional signal in pattern formation in plants. Proc. Natl. Acad. Sci. U S A **93**:9282–9286.

Wisniewska, J., Xu, J., Seifertova, D., Brewer, P.B., Ruzicka, K., Blilou, I., Rouquie, D., Benkova, E., Scheres, B., and Friml, J. (2006). Polar PIN localization directs auxin flow in plants. Science **312**:883.

Yan, S.S., Ning, K., Wang, Z.Y., Liu, X.F., Zhong, Y.T., Ding, L., Zi, H.L., Cheng, Z.H., Li, X.X., Shan, H.Y., et al. (2020). CsIVP functions in vasculature development and downy mildew resistance in cucumber. PLoS Biol. **18**:e3000671.

Zhang, J., Nieminen, K., Serra, J.A., and Helariutta, Y. (2014). The formation of wood and its control. Curr. Opin. Plant Biol. **17**:56–63.

Zhang, J., Eswaran, G., Alonso-Serra, J., Kucukoglu, M., Xiang, J., Yang, W., Elo, A., Nieminen, K., Damen, T., Joung, J.G., et al. (2019). Transcriptional regulatory framework for vascular cambium development in *Arabidopsis* roots. Nat. Plants **5**:1033–1042.

Zhu, Y.Y., Song, D.L., Xu, P., Sun, J.Y., and Li, L.G. (2018). A HD-ZIP III gene, PtrHB4, is required for interfascicular cambium development in *Populus*. Plant Biotechnol. J. **16**:808–817.

Plant Communications, Volume *2*

Supplemental information

Two MADS-box genes regulate vascular cambium activity and secondary growth by modulating auxin homeostasis in *Populus*

Shuai Zheng, Jiajia He, Zengshun Lin, Yingying Zhu, Jiayan Sun, and Laigeng Li

Supplemental Figures

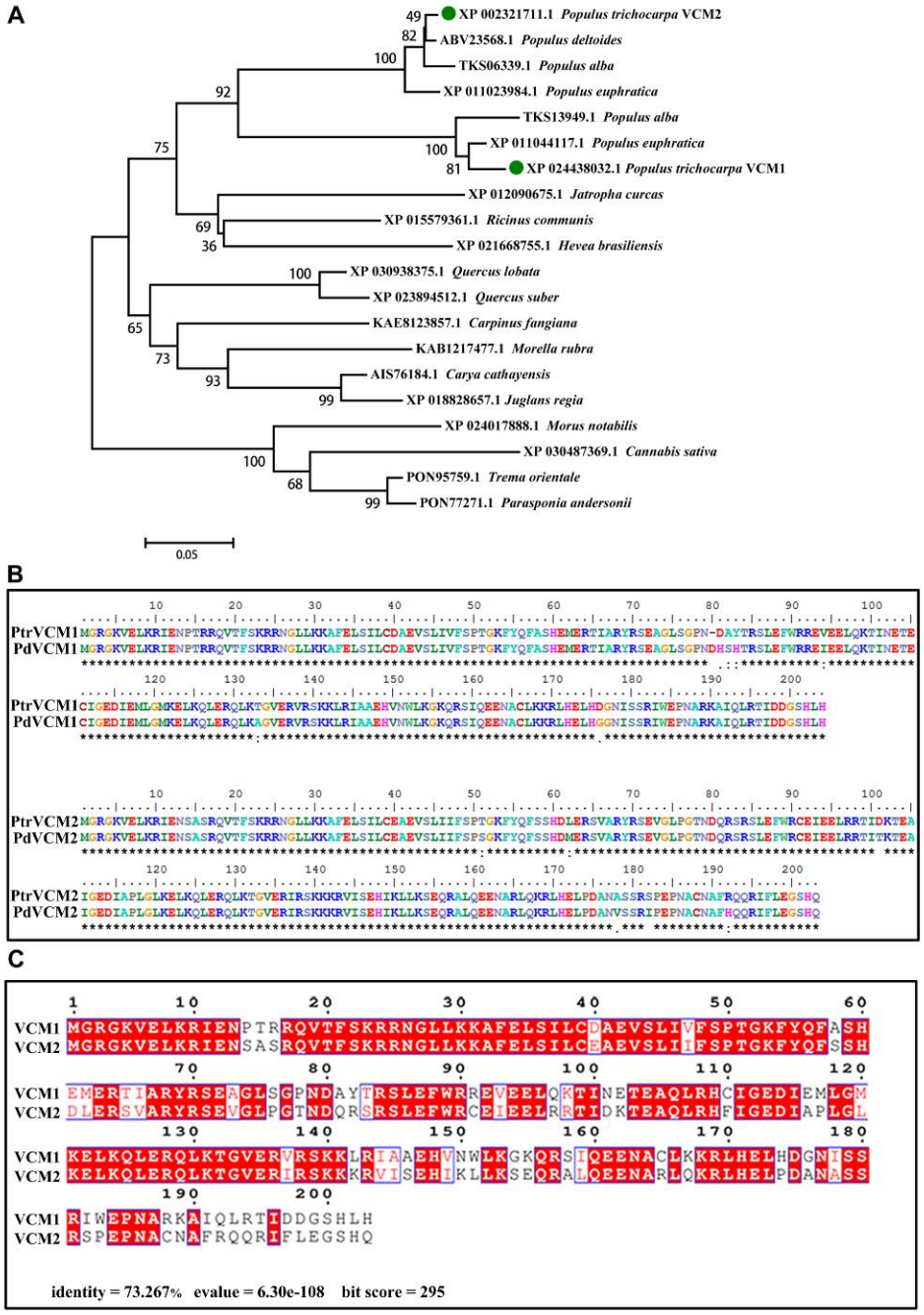

Figure S1. Phylogenetic analysis of *VCM1* and *VCM2*.
(**A**) A neighbor joining tree of *VCM1 and VCM2* and their homologs in various woody plant species. N. bootstrap = 1000. (**B**) VCM1 and VCM2 protein sequences from *Populus trichocarpa* and *Populus deltoides* × *P. euramericana* cv. 'Nanlin895'. (**C**) Similarity of *VCM1 and VCM2* protein sequences.

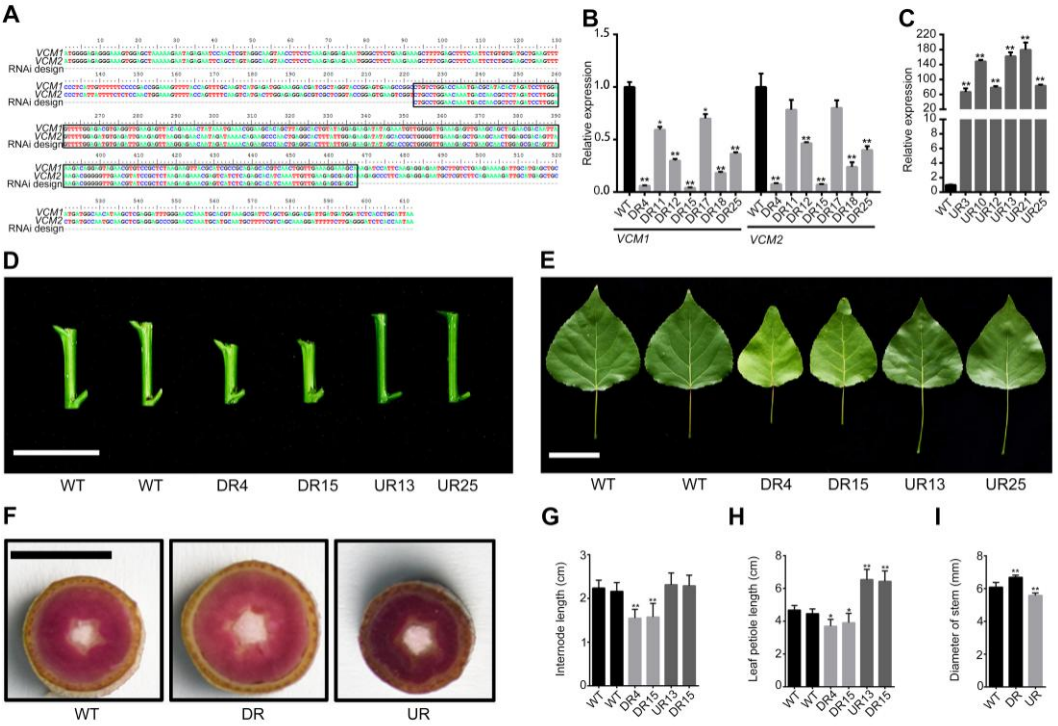

Figure S2. Regulation of *VCM1* and *VCM2* in *Populus*.
(**A**) RNAi fragment for downregulation of *VCM1& VCM2*. (B) A variety of *VCM1& VCM2* suppression in *DR* trangenics. (C) Expression of *VCM1* in *UR* trangenics. Values are means ± SD (n = 3 biological replicates). (D) The 10th internode of WT and transgenic, Scale bar = 2.5 cm. (E) Mature leaf from WT and transgenic, Scale bar = 5 cm. (F) Cross section of WT and transgenic, the position is 45 cm from the base in stem and plants were growth for more than five months. (G) Internode length (n = 10). (H) Leaf petiole length (n =10). (I) Stem diameter (n = 50). Statistical significance of differences was calculated based on two-tailed, two-sample student's t-test (**P <0.01, * P < 0.05).

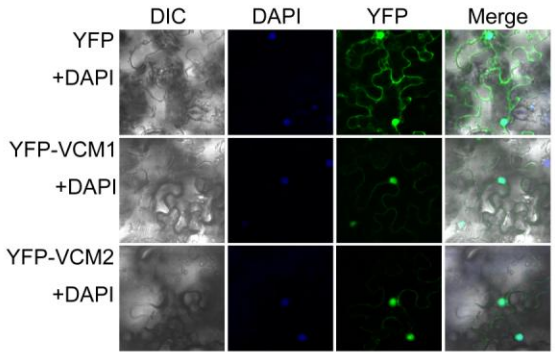

Figure S3. Subcellular localization of VCM1 and VCM2 in nucleus.
Localization of VCM1 and VCM2 was examined in tobacco leaf epidermal cells. YFP was fused with VCM1 or VCM2 to form YFP-VCM1 or YFP-VCM2. DAPI is used as a nucleus marker.

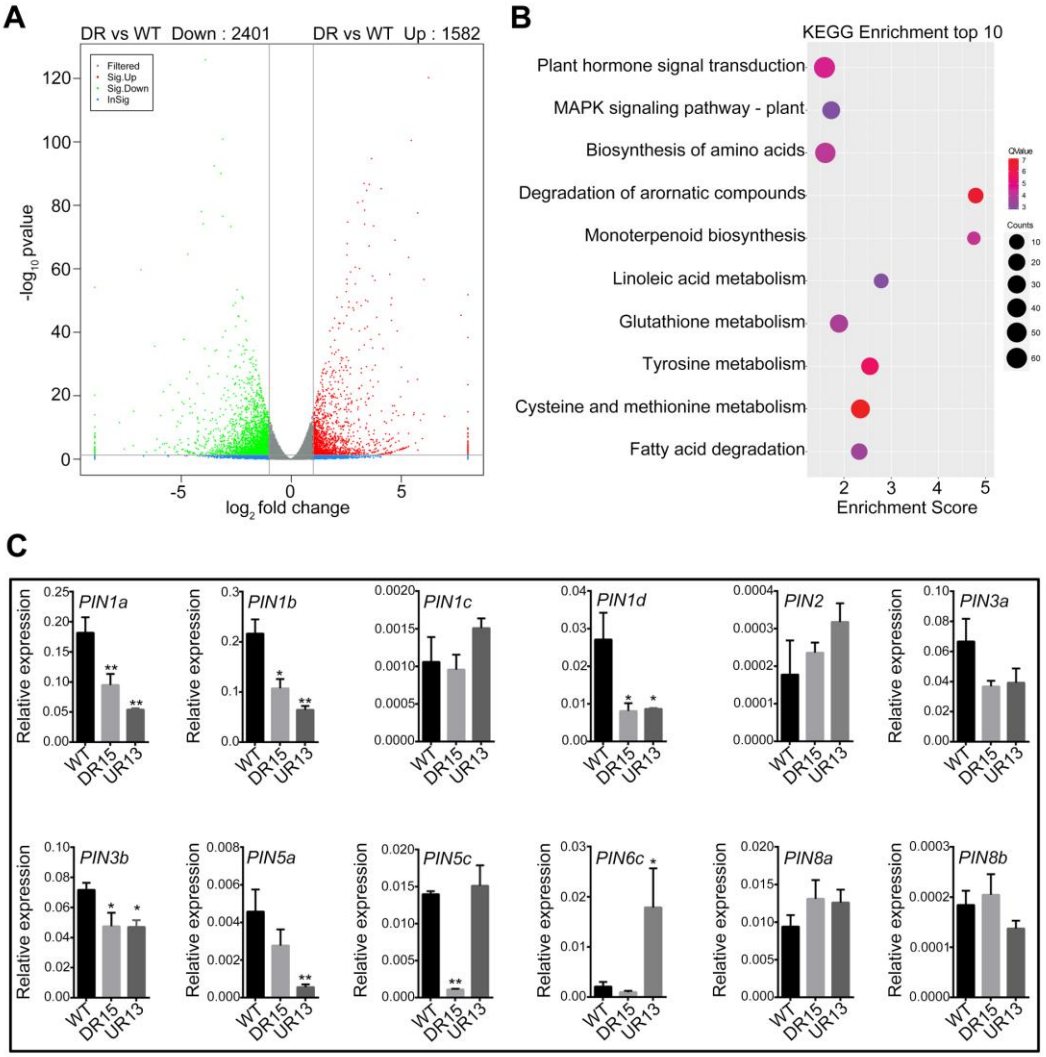

Figure S4. Differently expressed genes in downregulation of *VCM1& VCM2*.
(A) The transcriptome was substantially changed in downregulation of *VCM1&VCM2*. (**B**) KEGG enrichment shows the top 10 biological processes changed in the transcriptome. (**C**) qRT-PCR analysis of the *PIN* genes expression in regulation of *VCM1& VCM2*. Values are means ± SD (n = 3 biological replicates). Statistical significance of differences was calculated based on two-tailed, two-sample student's t-test (**P < 0.01, * P < 0.05).